Rare Metal Materials and Engineering
Volume 50, Issue 6, June 2021
Available online at www.rmme.ac.cn

Science Press

Cite this article as: Liu Kun, Wang Shuhuan, Feng Yunli, et al. Fabrication of $TbCu_7$-type Single Phase Sm-Fe-Zr-Nb Alloys by Melt-Spinning Combined with High-Energy Ball Milling[J]. Rare Metal Materials and Engineering, 2021, 50(06): 1950-1955.

ARTICLE

Fabrication of $TbCu_7$-type Single Phase Sm-Fe-Zr-Nb Alloys by Melt-Spinning Combined with High-Energy Ball Milling

Liu Kun, Wang Shuhuan, Feng Yunli, Zhao Dingguo, Zhang Yikun

College of Metallurgy and Energy, North China University of Science and Technology, Tangshan 063210, China

Abstract: The complete amorphous phase transformation of Sm-Fe-Zr-Nb alloy powders during high-energy ball milling process was investigated. The effects of milling time on the phase transformation and morphology of the Sm-Fe-Zr-Nb alloy powders were analyzed by X-ray diffraction, scanning electron microscopy, and high-resolution transmission electron microscopy. The result shows that complete amorphous microstructure is obtained after milling for about 2.5 h, and α-Fe phase (~5 nm) is precipitated from the amorphous matrix when the milling time is over 3 h. The number of short-range ordered structure increases. The uniform microstructure and the $TbCu_7$-type single phase are obtained by crystallizing the amorphous precursors milled for 2.5 h. The size of equiaxed grain is ~30 nm. This kind of micro-regulation plays a key role in improving the magnetic properties after nitriding.

Key words: high-energy ball milling; amorphous; phase transformation; energy barrier; annealing crystallization

High-performance permanent magnets (PMs) are widely used, especially in wind power generators, electric cars, and energy conversion devices[1-3]. $Sm_2Fe_{17}N_x$ with a rhombohedral Th_2Zn_{17}-type structure[4], and $SmFe_9N_x$ with a hexagonal $TbCu_7$-type structure[5], are promi- sing. The magnetic phase with a $Sm_2Fe_{17}N_x$ stoichiometry is stable, whereas $SmFe_9N_x$, a derivative of the P6/mmm $CaCu_5$-type structure with a certain pair of Fe atoms replacing samarium sites at random, is a metastable phase. When the alloy is subjected to a rapid non-equilibrated solidification process, the stable Th_2Zn_{17}-type structure transforms into the disordered $TbCu_7$-type structure. Both these phases are ferromagnetic and responsible for the excellent intrinsic magnetic properties of the magnet. However, compositional deviations and microstructural heterogeneities are unfavorable factors that cause the fluctuation of their magnetic properties. Although many research groups have attempted to directly obtain magnetic material with homogeneous microstructure and single phase by melt-spinning, the results are not satisfactory[6,7].

$SmFe_9$ and Sm_2Fe_{17} phases are normally formed by melt-spinning of Sm-Fe alloy. One method of obtaining an alloy with a homogeneous microstructure and single phase is to induce its crystallization from an amorphous alloy[8-10]. This requires the formation of complete amorphous structure of the alloy. A few research groups previously aimed to create Sm-Fe alloy ribbons with an amorphous microstructure directly by melt-spinning, but failed to obtain the expected results, especially the Sm-Fe binary alloy. This is because it is difficult to form its amorphous phase even when the wheel speed is greater than 60 m/s[11,12]. Based on the amorphous phase formation conditions, the negative mixing enthalpy of the system promotes the amorphous formation. Many researchers also attempted to add some high-melting metal elements, such as V, Zr, Nb, and Co[13-15], and to increase the wheel speed. However, no significant effect was observed. It is almost impossible to obtain completely amorphous Sm-Fe alloy only by melt-spinning process. High-energy mechanical ball milling is an effective method to obtain an amorphous microstructure[16].

In this study, the high-energy ball milling combined with melt-spinning process was adopted. The mixing enthalpy between Fe-Zr and Fe-Nb are -25 and -16 kJ/mol, respectively. It is negative and conducive to the formation of metastable phase and amorphous phase[17]. Then, Zr and Nb elements are added to promote the amorphous formation. The relationship between the phase transformation and milling time was established. The microstructure evolution mecha-

Received date: June 27, 2020
Foundation item: National Natural Science Foundation of China (51674123, 51774319); Hebei Natural Science Foundation (E2017209237)
Corresponding author: Wang Shuhuan, Ph. D., Professor, North China University of Science and Technology, Tangshan 063210, P. R. China, E-mail: wshh88@ncst.edu.cn

nism of Sm-Fe alloys during high-energy ball milling was clearly articulated by combining the experimental results and energy barrier theory. The powders with uniform microstructure and $TbCu_7$-type single phase were obtained by crystallizing the amorphous precursors, compared with direct melt-spinning, which is important in improving the magnetic properties after nitriding.

1 Experiment

Alloy ingots were prepared via the induction melting of elemental Sm and Fe under an Ar atmosphere; to compensate for the loss of Sm during the processing, excess Sm (~5wt%) was used. A small quantity of the prepared alloy ingots was placed in a quartz crucible with a lower orifice diameter of 0.8 mm and then re-melted via high-frequency induction heating under 101.325 kPa of 99.999% pure Ar. The melted alloy was then rapidly solidified into ribbons via melt-spinning, whereby the molten ingot was ejected onto a Cu wheel surface for rotating at 24 m/s. The chemical composition of the as-quenched ribbons was $Sm_{10.5}Fe_{82.1}Zr_{5.26}Nb_{2.1}$, which was determined by ICP. The $Sm_{10.5}Fe_{82.1}Zr_{5.26}Nb_{2.1}$ will be abbreviated to Sm-Fe-Zr-Nb, and applied to other places. The mixing enthalpy of Fe-Zr and Fe-Nb is negative, which is conducive to the formation of amorphous. Then Zr and Nb elements were selected. The ribbons were mechanically crushed into a coarse powder. The sieved Sm-Fe-Zr-Nb powders were further refined by high-energy ball milling under an Ar atmosphere for 0.5, 1, 2.5 and 3 h. The balls (6 mm in diameter) were made of 4400 MPa hardened steel. The mass ratio of the powder to the balls was 1:20. The milled powders were heat-treated at 700 ℃ for 20 min. X-ray diffraction (XRD; Cu-Kα, D8 ADVANCE) was used to determine the phase composition of the specimens. The morphology of the phases was analyzed by a transmission electron microscope (TEM; JEM-2100F) equipped with a cold cathode field-emission gun operated at the acceleration voltage of 200 kV. Specimens for HRTEM analysis were prepared by grinding the samples in an agate mortar with ethanol and depositing a few drops of the suspension on a Cu grid covered with a holey carbon layer.

2 Results and Discussion

XRD was used to confirm the phases of Sm-Fe-Zr-Nb alloy ribbons. Fig. 1 shows the XRD patterns of the as-quenched alloy ribbons and powders milled for 0.5, 1, 2.5 and 3 h. The results indicate that the as-quenched powder (milled for 0 h) consists of the $SmFe_9$ phase with excellent crystallinity and superstructure peak of the Sm_2Fe_{17} phase (arrow positions). No diffraction peak of α-Fe exists.

The XRD patterns of the milled powders (0.5, 1, 2.5 and 3 h) also reveal that when the milling time is 0.5 h, the metastable $SmFe_9$ phase, Sm_2Fe_{17} phase and an amorphous phase exist in the milled samples. The diffraction peak of α-Fe still does not exist. The Zr and Nb elements inhibit the precipitation of Sm_2Fe_{17} and α-Fe phases. With an increase in

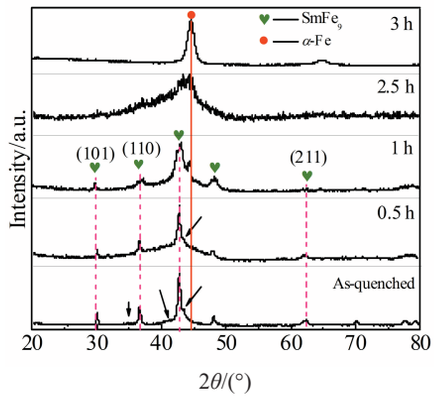

Fig.1 XRD patterns of Sm-Fe-Zr-Nb alloy powders milled for different durations

milling time from 0.5 h to 1 h, the diffraction peaks of $SmFe_9$ broaden, indicating that the $SmFe_9$ grains are refined and the content of the amorphous phase increases since the alloy receives sufficient energy. It can be seen from Fig. 1 (0~1 h) that the Sm_2Fe_{17} phase is completely transformed to $SmFe_9$ phase, which is due to the adding of Zr and Nb elements and the severe plastic deformation caused by high-energy ball milling. Therefore, the increase of dislocation density during the milling stage can promote the disordered atomic motion, and then accelerate the amorphization process. The diffraction peaks of α-Fe reappear, which may be caused by the volatilization of Sm during milling process, indicating that the α-Fe grains precipitate by absorbing the energy provided to the system and attract neighboring Fe atoms, leading to the concentration of Sm atoms around the α-Fe grains. When the concentration of Sm atoms approaches the eutectic composition of the Sm-Fe alloy, it favors the formation of the amorphous microstructure.

Upon increasing the milling time to 2.5 h, the XRD pattern only exhibits a strong diffuse scattering peak, and the diffraction peaks of other phases disappear, suggesting the formation of a complete amorphous structure. The volume fraction of the amorphous phase increases with increasing the milling time (0~2.5 h). When the milling time is up to 3 h, the diffraction peaks of α-Fe reappear and become sharp. These changes indicate the formation of an amorphous phase that coexists with the α-Fe phase and exists stably. Then, the optimum milling time was identified as 2.5 h. That kind of micro-regulation is beneficial to form an ultrafine equiaxed nanocrystal microstructure in the late crystallization stage.

Fig. 2 shows the morphology of the powders milled for 2.5 h, and the powder particle size distribution. The image of as-quenched ribbons is shown in the upper inset, and the size of the ribbons in the width direction is about 2 mm, and in the thickness direction it is about 20 μm (mean value of statistical results). The powder particle size milled for 2.5 h is ~3.26 μm, as shown in Fig.2b.

To clarify the phase structure of different samples milled for 0~3 h, the high-resolution TEM (HRTEM) micrographs are

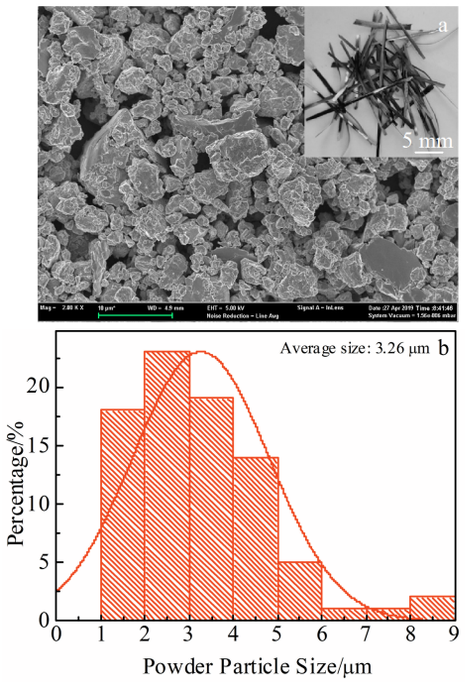

Fig.2 Morphology of Sm-Fe-Zr-Nb alloy ball-milled powders and as-quenched ribbons (inset) (a) and powder particle size distribution (b)

obtained (Fig. 3). The grain size of the as-quenched ribbon at the wheel speed of 24 m/s is large, and the distribution is non-uniform (Fig. 3a). The samples become completely amorphous until a milling time of 2.5 h, as shown in Fig. 3b (HRTEM image without any lattice fringe). The morphology of the powder milled for 3 h is shown in Fig. 3c. The powder milled for 3 h exhibits a mixture of amorphous and crystalline phases, and the corresponding SAED pattern is shown in the inset of Fig. 3c. The XRD patterns (Fig. 1, 3 h) was fitted with MDI Jade6.5, and the crystalline phase (black) content was measured. The volume fraction of amorphous phase and crystalline phase of the powder milled for 3 h is ~86% and 14%, respectively. The crystalline phase is the ultrafine equiaxed nanocrystals of α-Fe$_{(110)}$ with a diameter of approximately ~5 nm, which is determined in Fig. 3d, and the spacing of the stripes $d_{(110)}$ is 0.203 nm. The α-Fe phase is uniformly distributed in the matrix of the amorphous alloy phase (Fig. 3c), which agrees well with the XRD analysis results.

Fig. 4 is a scheme showing the mechanism of the transformation of microstructure, especially the decomposition of the amorphous phase when milled for 3 h, according to the results of the XRD and HRTEM analysis. It is well known that mechanical milling exerts a large amount of energy to the system and introduces numerous defects (i.e., vacancies and dislocations) in the microstructure of the milled powder, leading to its amorphization. When the milling time is up to 2.5 h, the complete amorphous microstructure is obtained. With an increase in the milling time, the energy of the system increases continuously, leading to the destabilization after complete amorphization is formed. Then, the number of short/medium-range ordered structure increases in amorphous alloy (<3 h). If increasing the system energy continuously (3 h), a small amount of α-Fe precipitates from the amorphous matrix. It can be assumed that

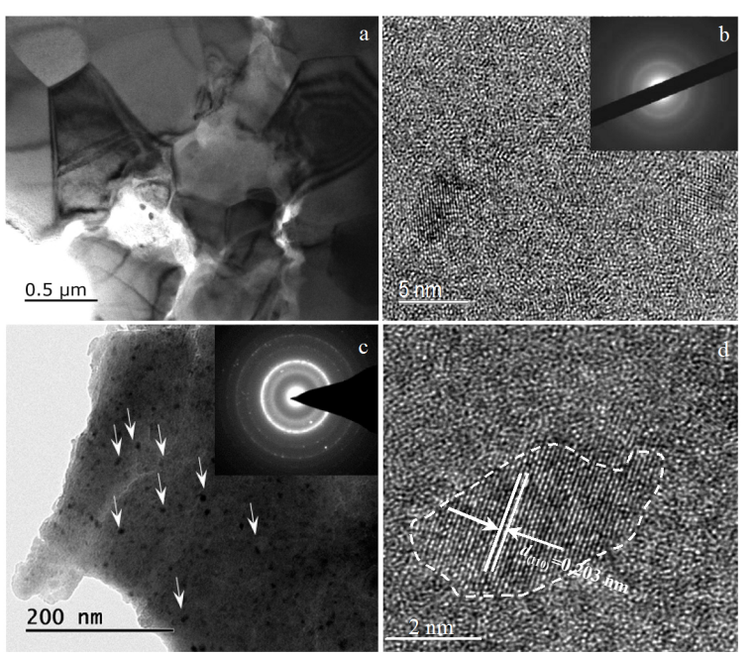

Fig.3 TEM (a, c) and HRTEM (b, d) images, SAED pattern (insets) of as-quenched ribbons (a) and Sm-Fe-Zr-Nb alloys milled for 2.5 h (b) and 3 h (c, d)

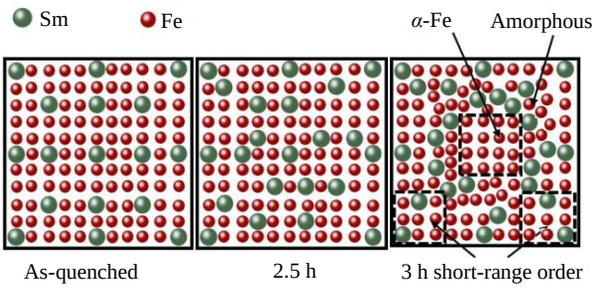

Fig.4 Schematics of microstructure evolution of alloy powder generated by different milling time

the ultrafine equiaxed nanocrystals of the α-Fe phases are precipitated by the coagulation or aggregation of the surrounding Fe atoms, resulting in the formation of a microstructure with amorphous phase (Sm-Fe) enveloping the α-Fe phase. This is because an increased content of Sm is favorable for amorphization. This migration leads to the formation of an α-Fe domain surrounded by a Sm-rich amorphous shell, as suggested by XRD and HRTEM results. The schematic of the microstructure evolution of the Sm-Fe alloy can give a deep understanding of the actual evolution process.

The amorphization of the as-quenched alloys can be explained by the reactions in Eq.(1~4). If the Sm content in the alloy before milling is sufficient, in the amorphization process, the stable Sm_2Fe_{17} phase absorbs energy and transforms into a metastable $TbCu_7$-type $SmFe_9$ phase and some Sm-rich domains; the $SmFe_9$ phase and Sm-rich domains then absorb energy and transform into a disordered amorphous phase. Therefore, during the amorphization process (<3 h), the samples mainly undergo reactions (1), and (2) as shown below. The relative proportion of reaction (2) increases with an increase in milling time to 2.5 h. As the milling time is increased further (3 h), the amorphous phase reaches an oversaturated, unstable and high-energy state. Then the samples undergo the reactions (3) and (4), the α-Fe grains are precipitated from the amorphous matrix, and accompanied by the growth of α-Fe nanocrystalline.

If the Sm content in the alloy before milling is not sufficient, the samples may undergo the reactions (1) and (2), but the redundant Fe atoms form the α-Fe phase, so a mixed microstructure of amorphous phase and α-Fe phase is formed. Therefore, a complete amorphous microstructure may not be obtained. To avoid the formation of α-Fe phase, we should ensure that the content of Sm in the amorphous microstructure is sufficient, and the milling time should be controlled at about 2.5 h.

$$Sm_2Fe_{17} \rightarrow SmFe_9,\ \Delta H_1 \quad (1)$$

$$SmFe_9 + \text{Sm-rich} \rightarrow \text{Amorphous},\ \Delta H_2 \quad (2)$$

$$\text{Amorphous} \rightarrow SmFe_9 + \alpha\text{-Fe},\ \Delta H_3 \quad (3)$$

$$\text{Small } \alpha\text{-Fe} \rightarrow \text{Large } \alpha\text{-Fe},\ \Delta H_4 \quad (4)$$

Therefore, the optimal milling time is set to ~2.5 h, at which the microstructure is completely amorphous with sufficient quantity of short/medium-range ordered structure. In subsequent crystallization annealing process, the step annealing was adopted through massive experimental contrast results. The milled powders were subjected to pre-annealing treatment at 490 ℃ for 90 min, and then crystallization treatment at 580 ℃ for 10 min. Fig. 5 is the diagram of the step annealing treatment process.

Fig.6 shows the XRD patterns of the as-quenched alloy and annealed powders. The as-quenched ribbons consist of the $SmFe_9$ phase with excellent crystallinity and superstructure peak of the Sm_2Fe_{17} phase (arrow position). After step annealing process, only 1:9 metastable phases exist.

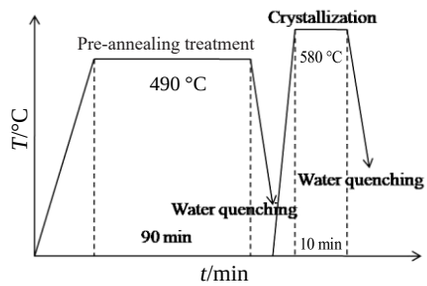

Fig.5 Diagram of step annealing process

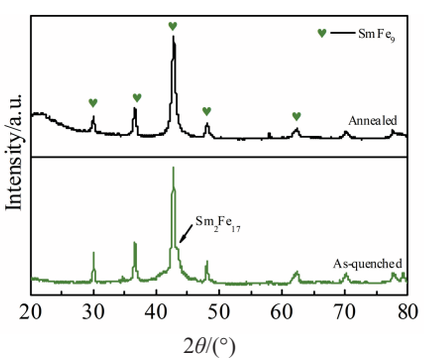

Fig.6 XRD patterns of the as-quenched alloy and annealed powders

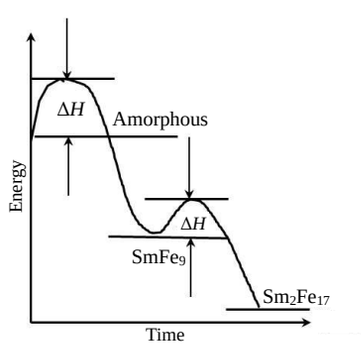

Fig.7 Energy barrier diagram of phase change

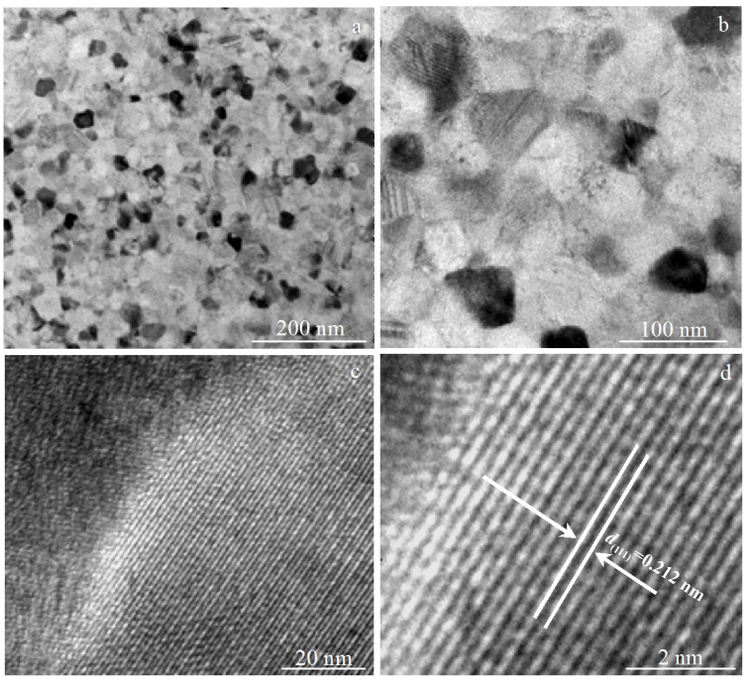

Fig.8 TEM (a, b) and HRTEM (c, d) images of annealed powders

The crystallization process can be explained by the energy barrier diagram, as shown in Fig. 7. The amorphous phase has a relatively high thermal stability and then requires higher activation energy to overcome the high energy barrier for crystallization. It is known that the metastable $TbCu_7$-type $SmFe_9$ phase has a higher energy than the stable Sm_2Fe_{17} phase. The short/medium-range ordered structure may form the $SmFe_9$ metastable phase and precipitate from the amorphous matrix in subsequent crystallization annealing process firstly. The transformation of $SmFe_9$ metastable phase to the Sm_2Fe_{17} stable phase needs to cross another barrier, and the continuous absorption of energy may further facilitate the formation of a more stable Sm_2Fe_{17} phase, as shown in Fig. 7. Therefore, the $SmFe_9$ phase is formed first, and the stable 2:17 phase can be converted from the 1: 9 phase only after the crystallization temperature is further raised. The single-phase 1:9 structure is obtained by step annealing process.

In Fig. 3a, the microstructure of as-quenched ribbons has been analyzed. The grain size is non-uniform, ranging from ~10 nm to ~200 nm. The microstructure of powders after step annealing treatment is shown in Fig. 8. The uniform microstructure is obtained by crystallizing the amorphous precursors (Fig. 8a and 8b), with the equiaxed grain size of ~30 nm. The stripe spacing is 0.212 nm, which is determined as the $TbCu_7$-type $SmFe_9$ phase, as shown in Fig. 8d.

3 Conclusions

1) The as-quenched powder of Sm-Fe-Zr-Nb alloy consists of the $SmFe_9$ phase and the Sm_2Fe_{17} phase. No α-Fe phase is presented. The Zr and Nb elements are beneficial to the formation of amorphous phase by inhibiting the precipitation of Sm_2Fe_{17} and α-Fe phases.

2) Complete amorphous phase can be obtained at the milling time of 2.5 h, and the number of short-range ordered structure increases, which is favorable to obtain an ultrafine and uniform crystalline microstructure in the subsequent crystallization annealing process. The uniform microstructure and the $TbCu_7$-type single phase can be obtained by crystallizing the amorphous precursors. The size of equiaxed grain is ~30 nm.

References

1 Adly A A, Huzayyin A. *J Adv Res*[J], 2019, 17: 103
2 Dorrell D G, Hsieh M F, Knight A M. *IEEE Trans Magn*[J], 2012, 48: 835
3 Ujihara M, Carman G P, Lee D G. *Appl Phys Lett*[J], 2007, 91(9): 93 508
4 Pandey T, Du M H, Parker D S. *Phys Rev Appl*[J], 2018, 9: 34 002
5 Lv B B, Yu D B, Zhang S R *et al*. *J Rare Earths*[J], 2013, 31: 979
6 Xing M, Han J, Wan F *et al*. *IEEE Trans Magn*[J], 2013, 49: 3248
7 Shi Y G, Hu C C, Zhou X G *et al*. *J Alloy Compd*[J], 2013, 563: 289
8 Kou X C, Qiang W J, Kronmüller H *et al*. *J Appl Phys*[J], 1993, 74: 6791
9 Tavoosi M. *J Therm Anal Calorim*[J], 2018, 131(2): 917

10 Saito T, Nishio D. *J Appl Phys*[J], 2015, 117(17): 752
11 Katter M, Wecker J, Schultz L. *J Appl Phys*[J], 1991, 70(6): 3188
12 Shkodich N F, Vadchenko S G, Nepapushevb A A *et al*. *J Alloy Compd*[J], 2018, 741: 575
13 Tozman P, Takahashi Y K, Sepehri-Amin H *et al*. *Acta Mater*[J], 2019, 178: 1016
14 Yan W L, Luo Y, Yu D B *et al*. *Rare Metals*[J], 2018, 37(3): 232
15 Saito T, Nishio-Hamane D. *AIP Advances*[J], 2018, 8: 56 230
16 Ghosh J, Mazumdar S, Das M *et al*. *Mater Res Bull*[J], 2008, 43(4): 1023
17 Saito T, Horita T, Nishio-Hamane D. *Mater Trans*[J], 2019, 60(7): 1384

熔体快淬与高能球磨法相结合制备$TbCu_7$型单相Sm-Fe-Zr-Nb合金

柳　昆，王书桓，冯运莉，赵定国，张一昆
(华北理工大学 冶金与能源学院，河北 唐山 063210)

摘　要：研究了Sm-Fe-Zr-Nb合金粉末在高能球磨过程中获得完全非晶态的相变过程。采用X射线衍射、扫描电镜和高分辨率透射电镜分析了研磨时间对Sm-Fe-Zr-Nb合金粉末的相组成及形貌的影响。结果表明：球磨2.5 h左右可得到完整的非晶态微观结构，球磨3 h以上，非晶态基体中析出尺寸约5 nm的α-Fe相，短程有序原子团数量增加。对球磨2.5 h后的非晶合金进行晶化处理后，得到了微观组织均匀的$TbCu_7$型单相合金，等轴晶尺寸约30 nm。该微观组织调控对改善氮化后的磁性能起关键作用。

关键词：高能球磨；非晶；相变；能量势垒；退火结晶

作者简介：柳　昆，女，1988年生，博士，讲师，华北理工大学冶金与能源学院，河北 唐山 063210，E-mail：79890799@qq.com